J. Fluid Mech. (2004), *vol.* 519, *pp.* 161–181.
DOI: 10.1017/S0022112004001181 Printed in the United Kingdom

On the relationship between the vortex formation process and cylinder wake vortex patterns

By DAVID JEON AND MORTEZA GHARIB

Graduate Aeronautical Laboratory, California Institute of Technology, Pasadena, CA 91125, USA

(Received 10 July 2004 and in revised form 12 July 2004)

The idea of vortex formation time, originally developed for vortex ring formation, is extended to bluff-body flows. Effects related to characteristic vortex formation time are shown for both the cylinder starting from rest and the cylinder undergoing forced oscillations in a steady flow. By looking at how wake vortices are formed when the cylinder is accelerated from rest, it is found that similarities exist between the formation process for wakes and for vortex rings. This formation process is then observed for forced oscillating cylinders, where the characteristic formation time interacts with the oscillation period. Frequently observed bluff-body phenomena will be recast in light of the vortex formation process.

1. Introduction

Considerable progress has recently been achieved in the understanding of the nature and characteristics of the wakes of cylinders. Williamson & Govardhan (2004) give a comprehensive review of wake pattern formation for oscillating and stationary cylinders. Gu, Chyu & Rockwell (1994) shed light on the formation of vortices in the near wake of oscillating cylinders. Explanations of wake behaviour are generally based on the interaction of fully developed vortices rather looking at where those vortices lie in terms of their formation process. Although studies of cylinders starting from rest do look at the initial formation stage of the wake vortices, these studies generally stop before the formation time becomes sufficiently large to have interesting effects. And for studies of cylinders in a steady free stream, the more typical approach is to study the interaction of vortices in the wake of the cylinder, rather than how those vortices formed. Following the methodology of Gharib, Rambod & Shariff (1998), an analysis of the vortex formation behind a cylinder was undertaken. The work is split into two parts: first, an examination of the initial formation process when a cylinder is accelerated from rest, followed by a study of how this formation process manifests itself in the case of the oscillating cylinder.

The flow behind a cylinder starting from rest is a canonical problem in the study of wakes. In addition, it is also a favourite for computational studies, perhaps because the initial conditions are clearly defined. Consider, for example, Honji & Taneda (1969), Bouard & Coutanceau (1980), or Koumoutsakos & Leonard (1995). However, like the vortex ring, most studies only looked at the early stages of development of this flow. When the cylinder begins to move, the wake is initially symmetrical and dominated by a pair of counter-rotating vortices. Usually, the studies focus solely on this regime of development. In an analogous manner, vortex ring studies are generally limited to rings of short formation time, when the vortex is compact. As shown in Gharib *et al.* (1998), interesting features of the formation process can be found by

extending the study to longer formation times. In this study, the evolution of the flow is studied well past the regime where the flow is nominally symmetrical – the equivalent of a cylinder wake of long formation time. Much as a vortex ring of indefinitely large formation times transitions into a jet, the wake of a starting cylinder eventually transitions into the classical von Kármán vortex street type configuration. In the first part of this paper, this transition and its relation to the vortex formation process will be discussed.

In contrast to the two flows mentioned above, the oscillating cylinder is a problem of more practical concern. The coupling of a bluff-body wake and its structure has been demonstrated to occur in a wide variety of manners. Of particular interest here is the situation where the vortex shedding process itself occurs at a frequency near to a resonant frequency of the structure (Parkinson 1989). A phenomenon known as lock-in can occur in this situation, where the wake is able to adjust itself to the structural frequency (Sarpkaya 1979). Such coupling can lead to large-amplitude vibrations of the structure, which can in turn lead to premature fatigue failure. This problem is typically understood in terms of modes of vortex shedding. One of the classical observations (Bishop & Hassan 1964) is that the lift force on the cylinder undergoes a nearly 180° phase shift at a frequency very near to the nominal shedding frequency of the stationary cylinder. Ongoren & Rockwell (1988) showed that the vortex shedding process also appears to flip in phase as well. Williamson & Roshko (1988) demonstrated that the wake patterns fell into distinct modes. In particular, on crossing the phase transition line, the wake appeared to switch from shedding two single vortices (known as the 2S mode) to shedding two counter-rotating pairs of vortices (2P mode). More recently, works by Gu *et al.* (1994) and Carberry, Sheridan & Rockwell (2001) have confirmed that the qualitatively observed behaviour persist when using quantitative vorticity measurements of the near wake. In the second part of this paper, the vortex formation process will be shown to link these various observations together. The interaction of the formation process and the motion of the cylinder will be shown to lead to a straightforward mechanism by which these transitions occur. Therefore, we intend to show how these disparate phenomena can be viewed as the product of one process, rather than having to resort to multiple mode and phase transitions to explain them.

2. Background

To summarize Gharib *et al.* (1998), the vortex formation process can be viewed as having three stages: initial vortex growth, saturation, growth of a trailing shear-layer-like structure. At early times, the separating boundary layer rolls up into a vortex, in a manner similar to the Kaden spiral (Saffman 1992; Pullin 1979). However, this process reaches saturation at some point, as the vortex cannot be of infinite size. Afterwards any additional vorticity in the separated boundary layer ends up in a shear-layer-like structure connecting the vortex back to the generator. If continued indefinitely, this trailing structure becomes the potential core of a jet. In this paper, the extension of this formation process to wake-type flows is proposed.

The qualitative change in the vortex should be appreciated first. This morphological change from compact, circular vortices to elongated vortical structures with trailing shear layers is key to understanding the formation process. In particular, as vortices are fed circulation by their generators, they do not grow indefinitely large. Rather the process saturates, after which the additional circulation does not enter the vortex itself but trails behind. The vortex then undergoes 'pinch-off', where it separates from the

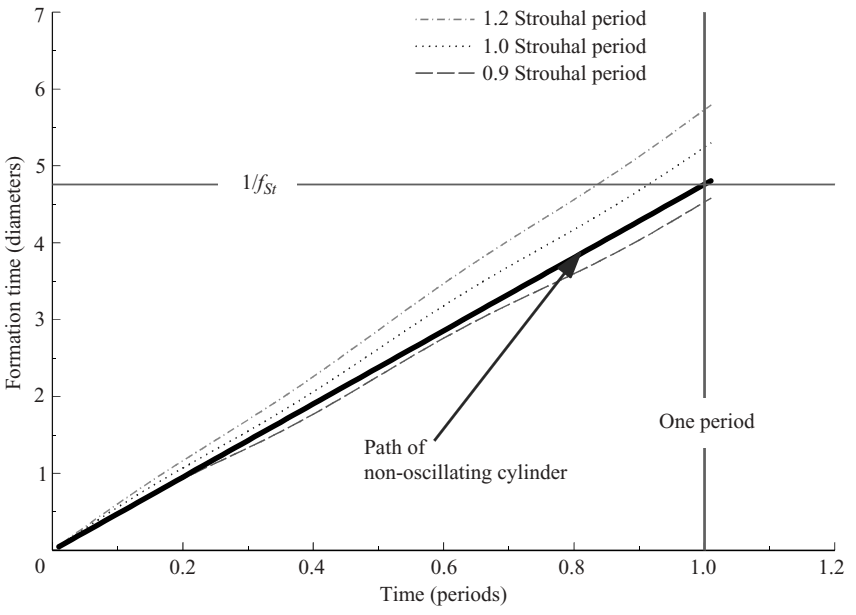

FIGURE 1. Distance travelled (i.e. non-dimensional time) by an oscillating cylinder during one shedding cycle with a transverse amplitude of 0.5 diameters. Within the lock-in region, the wake is phase-locked to the oscillating frequency. Therefore this is a simplistic measure of the formation time of the wake vortices as well.

boundary layer that provided its circulation. The details of the saturation mechanisms may vary (which leads to the vortex no longer accepting additional circulation), but this morphological change is a consistent identifier of this type of vortex formation.

Equally intriguing, the forming vortex appears to reach saturation at nearly the same non-dimensional time if the initial acceleration or final Reynolds numbers are varied. This led to the notion of a characteristic formation time, a natural pacemaker in the system dictating when saturation begins. For the vortex ring, the critical time is approximately four diameters, where time (t^*) is measured in terms of the average velocity of the generator and its diameter; this definition happens to be the same as the stroke ratio of the generator (ratio of the distance the generator travels divided by its diameter):

$$t^* = \frac{\overline{U}t}{d} = \frac{L}{d}. \tag{2.1}$$

Consequently, an analogous measure of time is used for the cylinder. In this case, time is scaled by the average velocity of the cylinder and its diameter. This, in turn, represents the distance the cylinder travels, in diameters.

For the forced oscillating cylinder, the equivalent time can be defined as the distance travelled per cycle, provided that the cylinder is oscillating in the lock-in region, where the vortex shedding is phase locked to the cylinder motion. This problem is, in some sense, an inverse one. Since the preferred shedding time is known (the inverse of the Strouhal number), the issue becomes what changes occur as a consequence of shedding either before or after this time. As a simple example, the path distance travelled by the cylinder is plotted in figure 1 for the case of a cylinder oscillating transversely at an amplitude of 0.5 diameters. The x-axis is time (measured in periods) and the y-axis is the path distance travelled (measured in diameters). The solid line

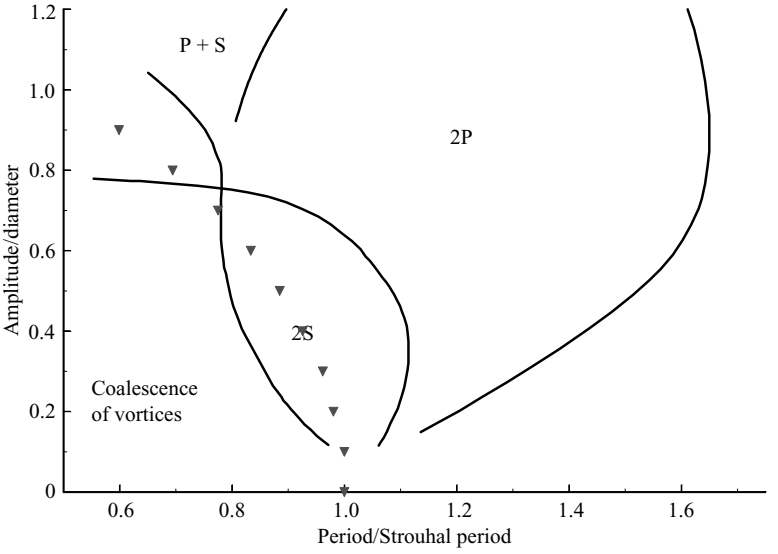

FIGURE 2. Transition point based on the simple model of path distance travelled by the oscillating cylinder. The triangles represent the locations on the Williamson–Roshko wake mode map where the path distance of the oscillating cylinder equals that of a non-oscillating cylinder. For details of what the various modes look like, refer to the original Williamson & Roshko (1988) paper.

corresponds to the case of the non-oscillating cylinder – a straight line with slope $1/St$. For oscillation frequencies in the lock-in range, the wake frequency follows the oscillation frequency of the cylinder; hence, the shedding time of the oscillating case depends on the frequency of motion. For frequencies above the Strouhal frequency, the path distance can actually be less than for the non-oscillating case. In this simple model, the frequency at which the path distance is equal to the inverse of the Strouhal number corresponds to saturation in the wake formation process, since that is where the cylinder would have travelled the same distance per vortex shedding as the non-oscillating cylinder. Neglecting the additional acceleration due to oscillation, it is presumed that an oscillating cylinder would therefore shed a vortex when its path distance equals the inverse of the Strouhal number. The frequency at which the path distance equals the inverse of the Strouhal number is plotted in figure 2 for a range of oscillation amplitudes, overlaid upon the Williamson & Roshko mode map. Although the frequency does not lie on the 2S–2P transition curve, it is close – especially for such a simplistic model. More importantly, it suggests that a formation-time-type transition may occur in this region, one where vortex satuation and vortex formation time play a role in wake behaviour. Therefore we will see if the observed wake transitions – like those seen in Williamson & Roshko (1988) and Ongoren & Rockwell (1988) – can be recast in terms of vortex formation time.

As an additional note, it is worth speculating on whether or not the value of the Strouhal number is directly connected to the vortex formation time. If we can observe vortex formation time effects that hinge around a formation time of $1/St$, it would be natural to conclude that the value of the Strouhal number is in fact set by the vortex formation time. Therefore understanding the timing of the vortex formation process can be the way to understand why the Strouhal number is so remarkably constant, even across differently geometries and wide ranges of Reynolds number.

3. Experimental set-up

These experiments were performed in two separate facilities. The starting flow experiments were conducted in the GALCIT X-Y Towing Tank facility. This consists of a large glass tank, approximately 4.5 m long and 1 m wide, with optical access from all sides. The tank was filled to a depth of approximately 50 cm of water, resulting in a typical aspect ratio of 20. To minimize three-dimensional effects, the free end of the cylinder was held around 0.05 diameters from the floor, supported from above in a cantilever fashion. Atop this tank is mounted a two-axis traversing system capable of towing the cylinder down the length of the tank. The traverse is computer controlled, allowing us to precisely specify the acceleration profiles used in the starting the cylinder flow.

The oscillating cylinder experiments were conducted in a low-speed, free-surface water tunnel facility. This tunnel has a glass test section, about 45×55 cm in cross-section. A two-axis, computer-controlled traversing system was used to move the cylinder in arbitrary two-degree-of-freedom patterns in a steady free stream. Again the cylinder was supported in cantilever fashion from above; in this case, the free end was placed around 0.5 diameters from the floor, to match the boundary layer thickness on the bottom surface of the facility. Aspect ratios varied between around 20 and 50 for these cases.

In both cases, the primary diagnostic technique was digital particle image velocimetry (DPIV). For these experiments the images were taken using a video camera and interrogated using cross-correlation. See Willert & Gharib (1991) for more details on DPIV. For the starting flow case, a continuous argon-ion laser was mounted beneath the tank and the beam was formed into a sheet in a plane parallel to the floor. A mechanical chopper, synchronized to the video signal, was used to produce pulses of light at known intervals. The camera was attached to the traverse moving the cylinder and hence moved with the cylinder. For the oscillating cylinder case, a pair of Nd:YAG pulsed lasers were used. Again the light sheet was formed in the plane parallel to the floor. The camera viewed the flow from beneath the test section through a mirror arrangement.

In both cases, the data were processed with a window size of 32×32 pixels with a step size of 8×8 pixels. We then used a discrete-window-shifting algorithm with spatial filtering to reduce noise and effectively decrease the window size to 16×16 pixels. The window size is between 0.13 and 0.17 diameters. Error in PIV measurements is affected by the nature of the flow itself (for example, high gradients skew the results). However, in laboratory testing, our PIV processing software delivers around 1–5% error in the velocity data, and about 5–10% error in the vorticity.

4. Starting cylinder

The vortex formation process for the starting cylinder wake begins when the initially attached boundary layer on the cylinder separates. A cylinder, initially at rest, is quickly accelerated up to a constant velocity, typically at constant acceleration. The separated boundary layers rolls up into vortices and begins to move into the wake. As the vortices are fed vorticity from the boundary layer, they continue to grow roughly symmetrically. At a later time, the wake undergoes a transition and starts to become strongly asymmetrical. This flow is loosely analogous to the vortex ring, except that a momentum sink is turned on at some time instead of a momentum source. (Here momentum source and sink are analoguous to their use in potential flow.) Consequently, the details of the formation process differ, but not the general

pattern. After an overview of the flow at early time, the details of the formation process will be examined. The growth of asymmetry, coming from an instability of the symmetrical flow, will be shown as a likely mechanism controlling the formation and saturation process. In the next section, we will use the ideas of short and long formation time shown here to explain the dynamics of the oscillating cylinder wake.

A snapshot of the cylinder flow at early time is presented in figure 3. For this discussion, time is measured in terms of the number of diameters the cylinder has travelled from its initial position; this time scale tends to minimize the effects of different initial acceleration profiles. In this particular case, the final cylinder Reynolds number is 2000 and the final velocity is reached in 1.5 diameters from rest. (In real units, this case represents a 2.54 cm cylinder accelerating to 7.87 cm s^{-1} in 2 s; the fluid is industrial lab water.) At very early times (less than four diameters), the wake remains very symmetrical, consisting primarily of two large vortices in the near wake. At later times, the wake becomes asymmetrical and eventually sheds a vortex. Thereafter, the wake gradually enters a nearly periodic shedding state. Around a time of four diameters, a transition occurs between the two states, from the initially symmetrical to the asymmetrical. Note however that for sufficiently low initial acceleration, this pattern does not manifest itself. (The exact critical acceleration depends greatly upon Reynolds number and background noise. For example, in a well-resolved DNS computation, the wake may never become asymmetrical before numerical errors accumulate.) Rather, the symmetrical state appears to gradually fade into Kármán vortex shedding instead of going through a dramatically asymmetrical state first. This can be seen in figure 4; this is presented simply to point out how the process changes at very low acceleration, and will not be discussed further.

Using a methodology similar to Gharib *et al.* (1998), the circulation of the growing vortices is measured as a function of time. In every data frame, the total circulation was measured by taking the area integral of the vorticity field where the vortex was visibly located. Care was taken to ensure that only the vorticity in the vortex was counted as the circulation. The circulation is scaled by the circulation of the first shed vortex, immediately after it is shed. (The first shed vortex is the first vortex that separates from the cylinder and moves independently downstream. This vortex may come from either side of the cylinder. It is believed that this vortex contains the critical amount of circulation, which is why it is shed in this manner. In the vortex ring study, the equivalent of the first shed vortex is the vortex ring itself.) The results are shown in figure 5. This is a composite plot of four runs, all at Reynolds number of 1000, but with initial acceleration ramps ranging from 0.5 s to 2.0 s (0.3 to 1.5 diameters). The vortex formation time is defined as the time when the circulation of the wake has reached the level of that which ends up in the first shed vortex; in other words, when the non-dimensional circulation reaches 1. By coincidence, the cylinder wake seems to have the same formation time as the vortex ring – four diameters. It would appear that a similar saturation event occurs in the cylinder wake. It is worth noting that this number is not close to 4.8, which would be the Strouhal period. We believe this arises from the extra vorticity flux coming from the cylinder acceleration, which is not present for steady cylinder motion.

Not only does the circulation growth share the vortex ring's pattern, but also the vortex morphology. Recall that the vortex ring begins life as a compact vortex with a very thin shear layer connecting it back to its generator. After saturation, the vortex begins to move away and the remaining circulation ends up in a trailing

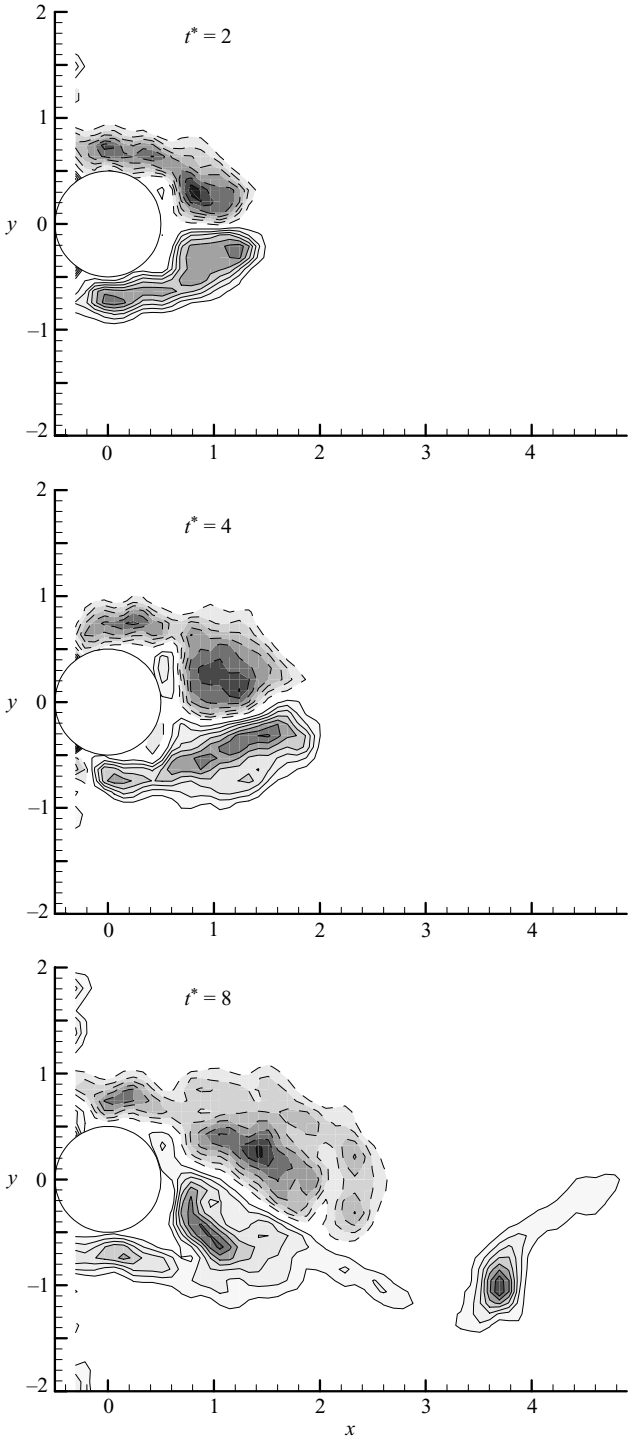

FIGURE 3. Initial wake behind a cylinder starting from rest. Time is non-dimensionalized by the diameter and the average cylinder velocity – equivalently, the distance travelled in diameters. Contours are non-dimensional vorticity levels of -7, $-6 \ldots 7$. On this and similar figures negative levels are shown as dashed lines, zero vorticity is white and deeper grey denotes larger magnitude.

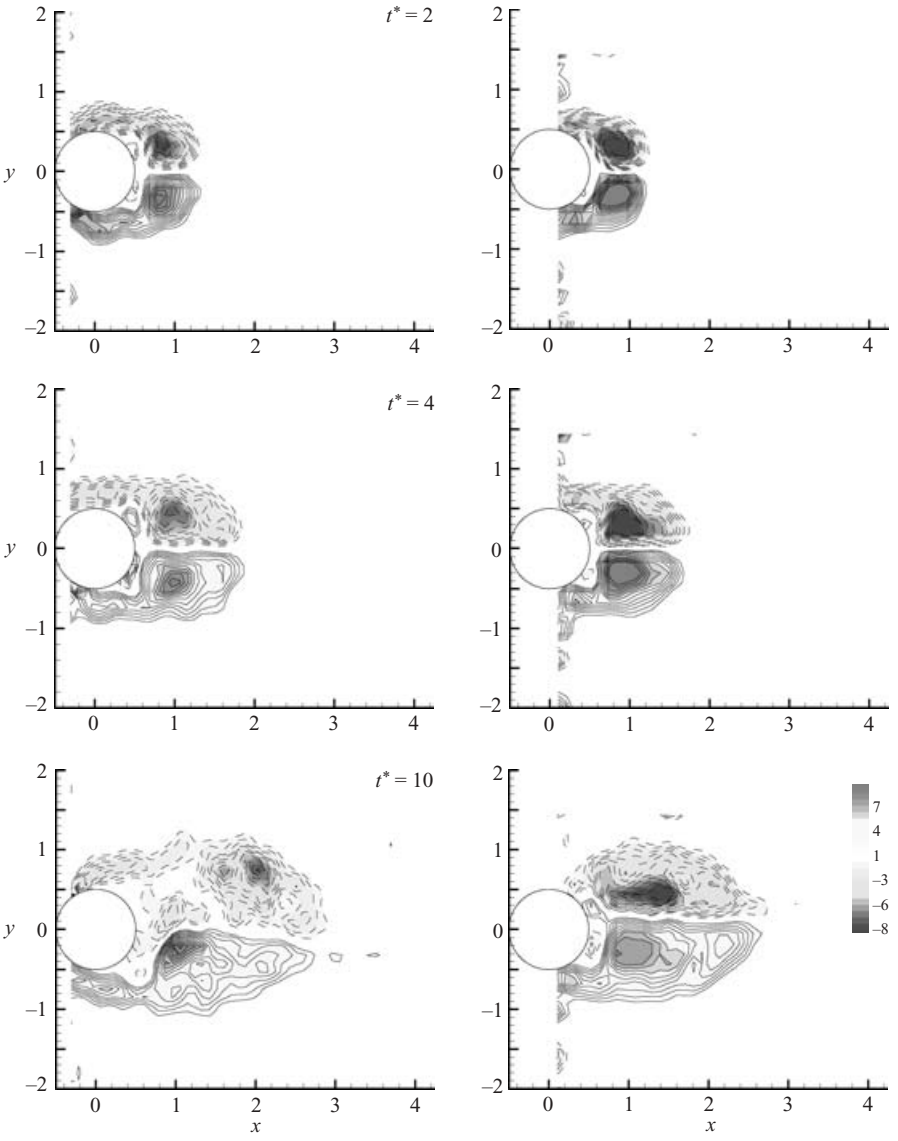

FIGURE 4. Comparison of wake development at two different initial accelerations. On the left is a case above the critical acceleration, on the right, below. Note how the lower acceleration case retains the initial symmetry to long times. Contours are non-dimensional vorticity levels of -8.5, $-7.5 \ldots 8.5$.

jet-like structure. In the case of the cylinder, the same pattern exists. The early time ($t^* = 2$) compact symmetrical state gives way to an intermediate ($t^* = 4$) elongated vortex. This structure splits and the wake sheds a vortex whose circulation is equal the circulation of the whole vortex around time four diameters. This morphological transition is important when we come to consider oscillating cylinder flows in § 5.

To better study this transition, the asymmetry of the wake was measured. In principle, this can be done by decomposing the wake into orthogonal modes and measuring the power in the asymmetrical modes. R. Henderson (1995, personal

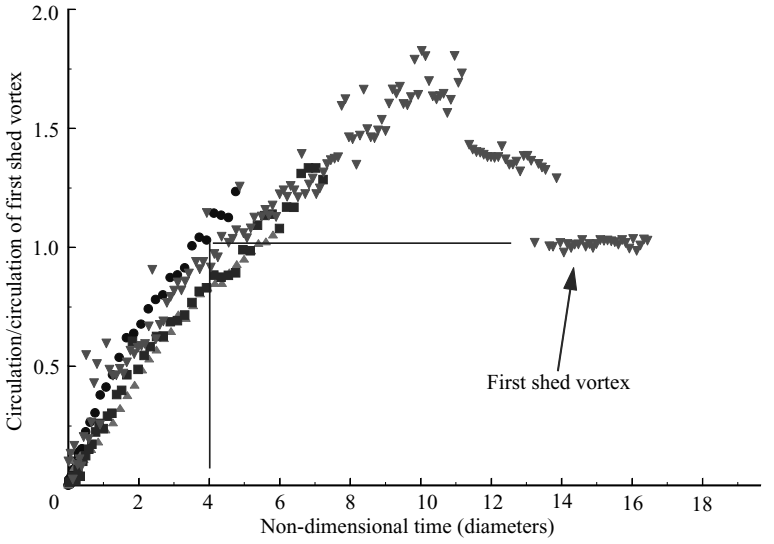

FIGURE 5. Circulation in the wake of the starting cylinder, normalized by the circulation of the first shed vortex, as a function of non-dimensional time (i.e. distance travelled). Different symbols refer to different acceleration profiles.

communication) suggested, as a simple alternative, that the wake could be divided into two parts, one of which was mirror symmetrical about the wake centreline and the other being everything else. For example, the symmetrical part is that which has a streamwise component of velocity of the same sign above and below the axis of symmetry and opposite sign for the transverse component. Since the wake at very early times is nearly mirror symmetric about the centreline, growth of the other mode should be an indicator of wake asymmetry. The norm of the asymmetrical part, computed by taking the vector norm of the velocity magnitudes, is considered to be the measure of asymmetry of the flow field. The resulting decomposition is shown in figure 6, where the contours represent the local magnitude of the respective modes. At time two diameters ($t^* = 2$), virtually all of the flow is in the symmetrical state, as expected. Around time four diameters ($t^* = 4$), a significant region of asymmetry has formed where the two main vortices touch. By time eight diameters ($t^* = 8$), the asymmetrical mode has nearly the same magnitude as the symmetrical state in the near-wake region. In figure 7 the norm of the asymmetrical mode is plotted on semi-log axes. (Norms are computed in the usual sense. For example the 1 norm is sum of the absolute values of the mode.) At early times, the measurement is probably noise limited, but shows a low level of asymmetry. Around time four diameters, the asymmetrical mode experiences nearly exponential growth before saturating at late time as the flow transitions towards shedding. Readers might note that the peak in the asymmetry curve is nearly coincident with the peak in the circulation and wonder if there might be a connection. In general, while the behaviour at $t^* = 4$ is quite consistent, this is not the case near where asymmetry and circulation peak. Presumably this is because the wake is most nonlinear around that transition time and small details matter more. Regardless, it would appear that an instability in the flow triggers the growth of asymmetry in the wake, which in turn switches the wake from the initial symmetrical to the Kármán shedding state.

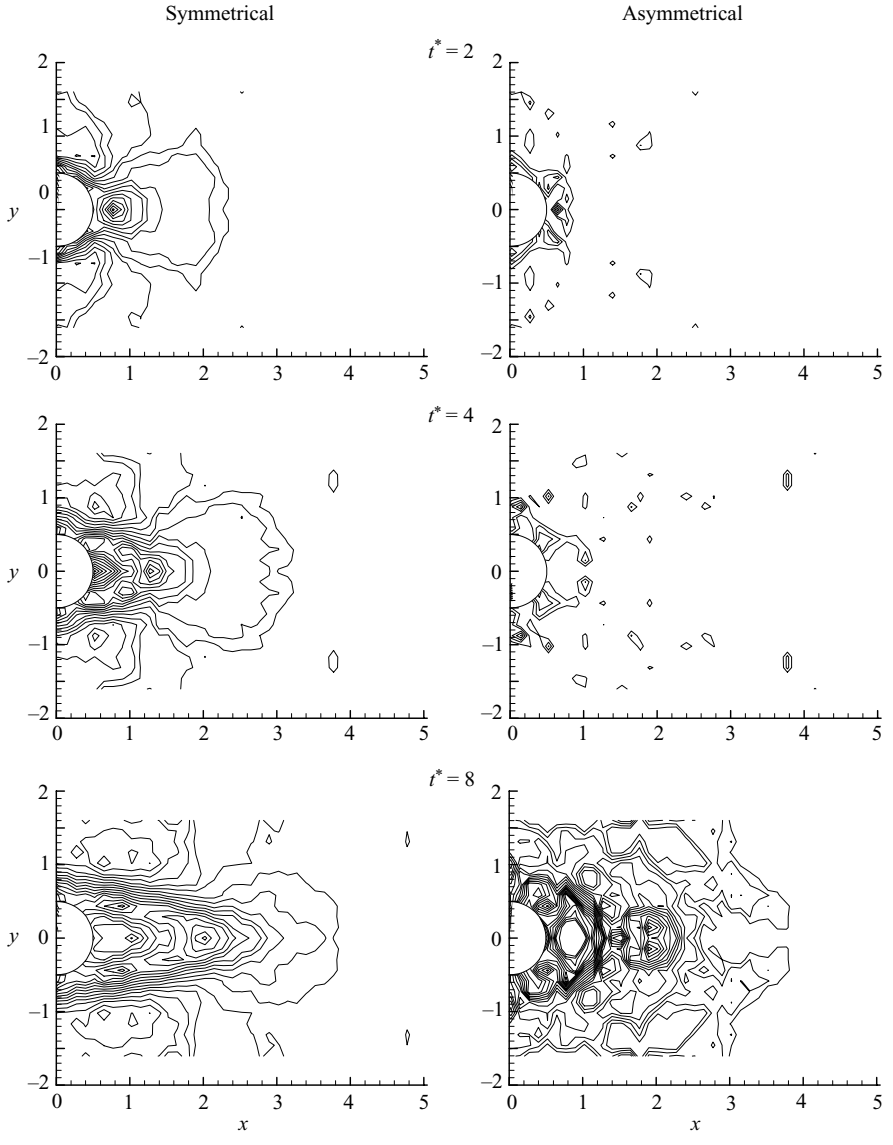

FIGURE 6. Symmetric and asymmetric components of the wake of a starting cylinder. Contours denote magnitude. Contours are 0.1, 0.2 . . . 2.5 on the symmetrical side, and 0.1, 0.15 . . . 1.0 on the asymmetrical side.

5. Oscillating cylinder

Like the starting cylinder, the oscillating cylinder flow has been studied for a long time. Of particular interest here is the phenomenon of vortex-induced vibration. Researchers have extensively mapped the response of simple geometries (like cylinders and prisms) to changing flow conditions. The results have traditionally been explained in terms of mode changes in the wake. (Consider Brika & Laneville 1993, especially, figure 19.) Our goal is to offer an alternative view on why these wake changes occur, one based of the concept of vortex formation time. We will now attempt to portray

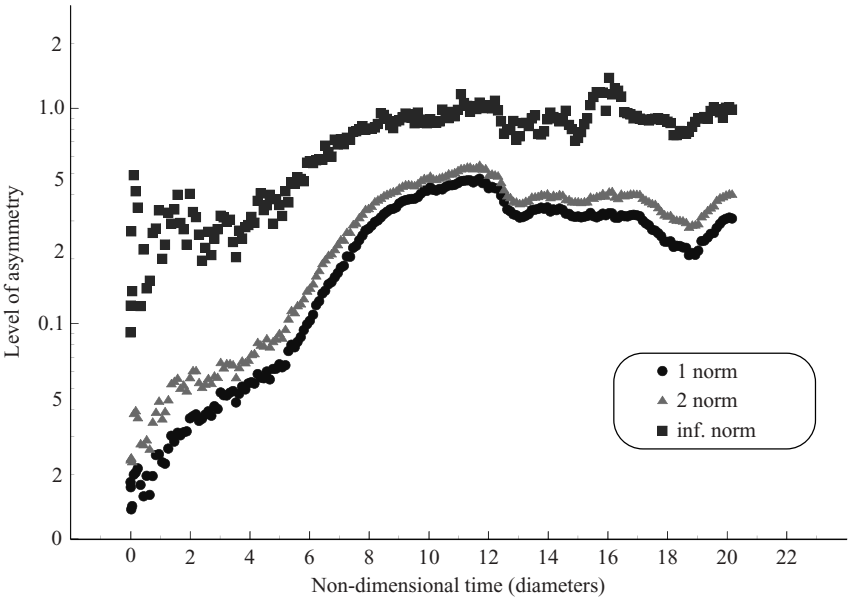

FIGURE 7. Growth of the norm of the asymmetrical mode of the wake with time. On this semi-log plot, the nearly linear growth between times 4 and 8 imply an exponential growth of asymmetry.

the behaviour of the oscillating cylinder's wake in terms of concepts learned from the study of the starting cylinder case. We shall see that looking at the wake behaviour in terms of short and long formation time effects will clarify a range of previously noted effects under a simple unifying model. Although the base flows are quite different, the underlying mechanisms that affect the formation of vortices remains the same for the two flows. Seeing how wake vortices form under the controlled conditions of the starting cylinder flow will make it easier to understand how the same processes are present in the oscillating case.

To illustrate the behaviour of the wake of a forced oscillating cylinder, two sets of vorticity plots are shown in figures 8 and 9. In both cases, non-dimensional vorticity fields (scaled by the free-stream velocity and cylinder diameter) are phase-averaged and plotted for six phases in the upper half of the cylinder motion. In our phase time, the cylinder is moving downward during phases 4/12 to 9/12, and moving upward between phases 10/12 to 3/12. Phase time is linked only to the transverse motion, and any streamwise motion is always relative in phase to the transverse. In these figures, the cylinder was forced in sinusoidal motion in both the streamwise and transverse directions simultaneously. The streamwise motion has twice the frequency of the transverse and no phase difference, so that the motion would draw a figure-eight pattern if one were moving with the cylinder. In figure 8, the cylinder is oscillating at 0.84 Strouhal periods (hence has a formation time less than that of the non-oscillating cylinder), with a transverse amplitude of 0.5 diameters. The streamwise motion is about 0.1 diameters, with zero phase difference between the two directions. This produces a wake similar to regular von Kármán shedding, albeit with a very short wake. In contrast, figure 9 is for a similar motion, except that the transverse motion was at 1.2 Strouhal periods (therefore with a formation time longer than that of the non-oscillating cylinder). The streamwise motion is not important at this time;

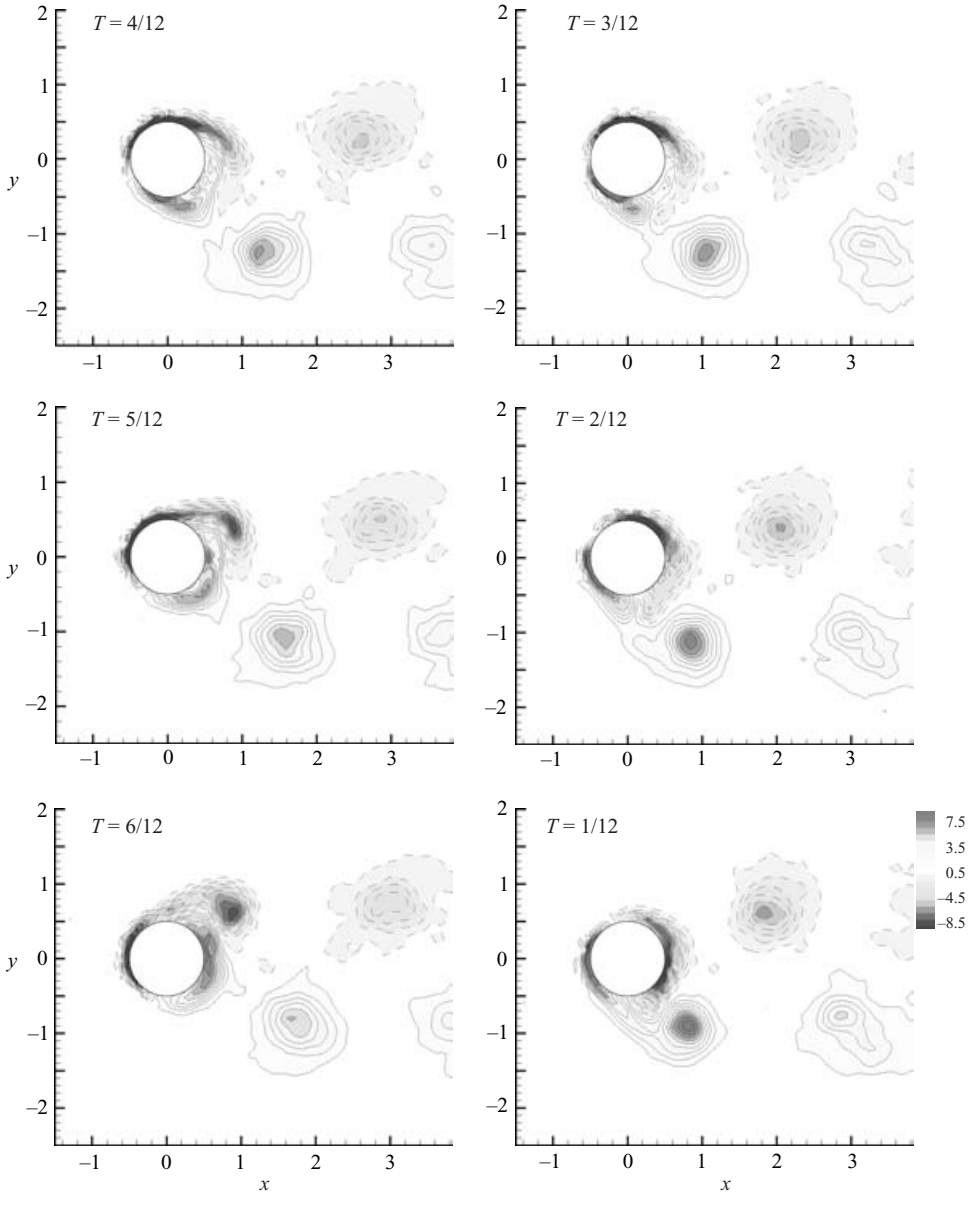

FIGURE 8. Wake of an oscillating cylinder for the upper half of motion. T refers to the phase time (from 1/12 to 12/12). Reynolds number is 1100, transverse period is 0.84 the nominal Strouhal period, transverse amplitude is 0.5 diameters, streamwise amplitude is 0.1 diameters, and the relative phase between the two is 0. Contours are non-dimensional vorticity levels of -8.5, $-7.5 \ldots 8.5$.

we are using these figures because they are representative of the changes that the wake undergoes without the additional factor of mode change involved. (However, in a later section, we will illustrate how streamwise motion affects the appearance of the wake.) Although the wake is nominally shedding one vortex per side per cycle, it is qualitatively different from the wake at higher oscillation frequency. Note especially the much longer wake with the elongated shear layer: this feature is also present

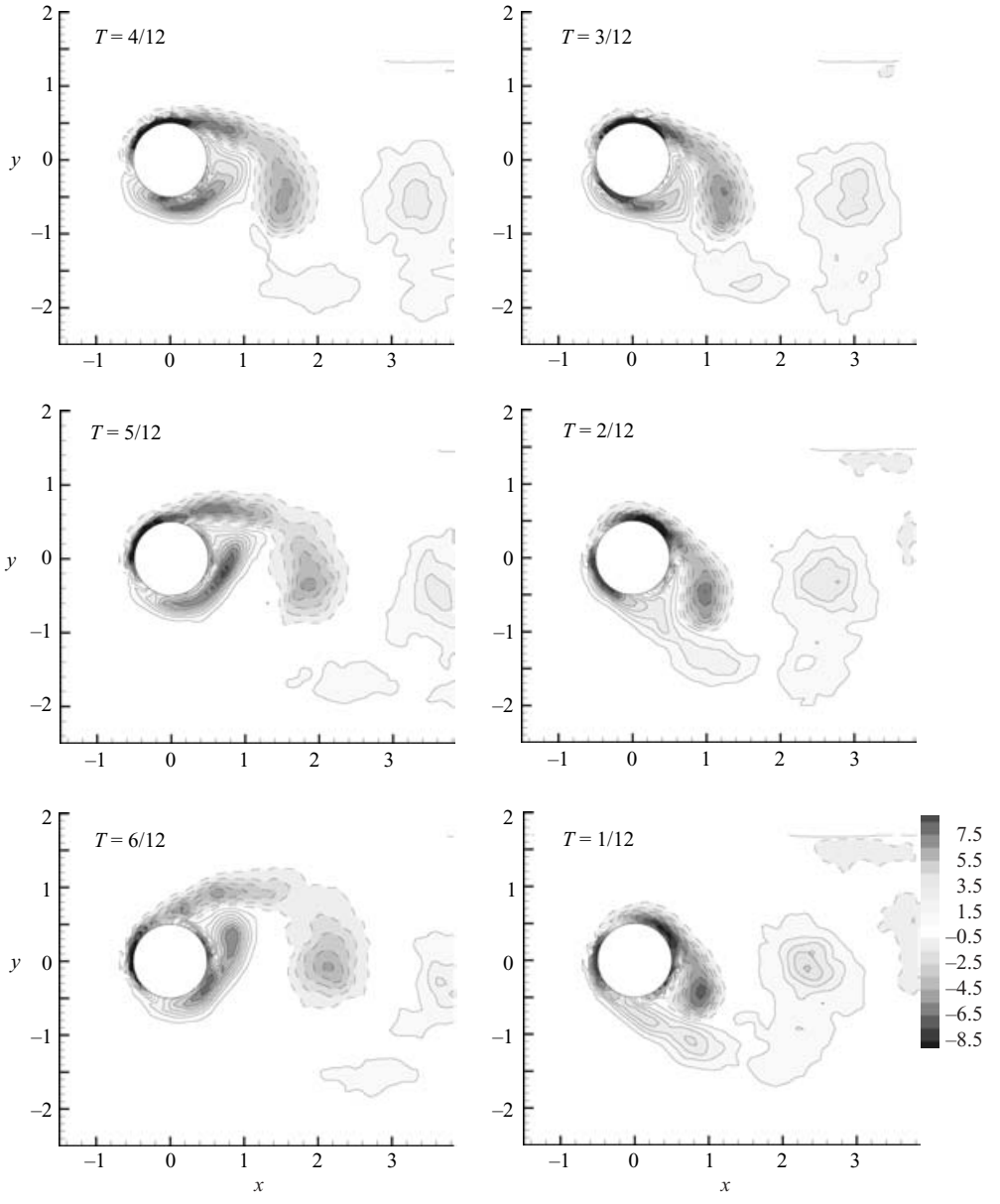

FIGURE 9. As figure 8 but Reynolds number is 1500, transverse period is 1.2 the nominal Strouhal period.

in the 2P mode. Other researchers have documented similar changes in the wake (albeit without the streamwise motion). Carberry *et al.* (2001) and Govardhan & Williamson (2001) offer similar plots of oscillating cylinder wakes; the change from compact vortex to vortex with elongated shear layer is apparent in their plots as well.

In figure 10, the three classes of flow are presented side-by-side. Notice the characteristic change in vortex morphology as formation time increases. In every case, there is a change from a compact vortex to a vortex attached by a long shear

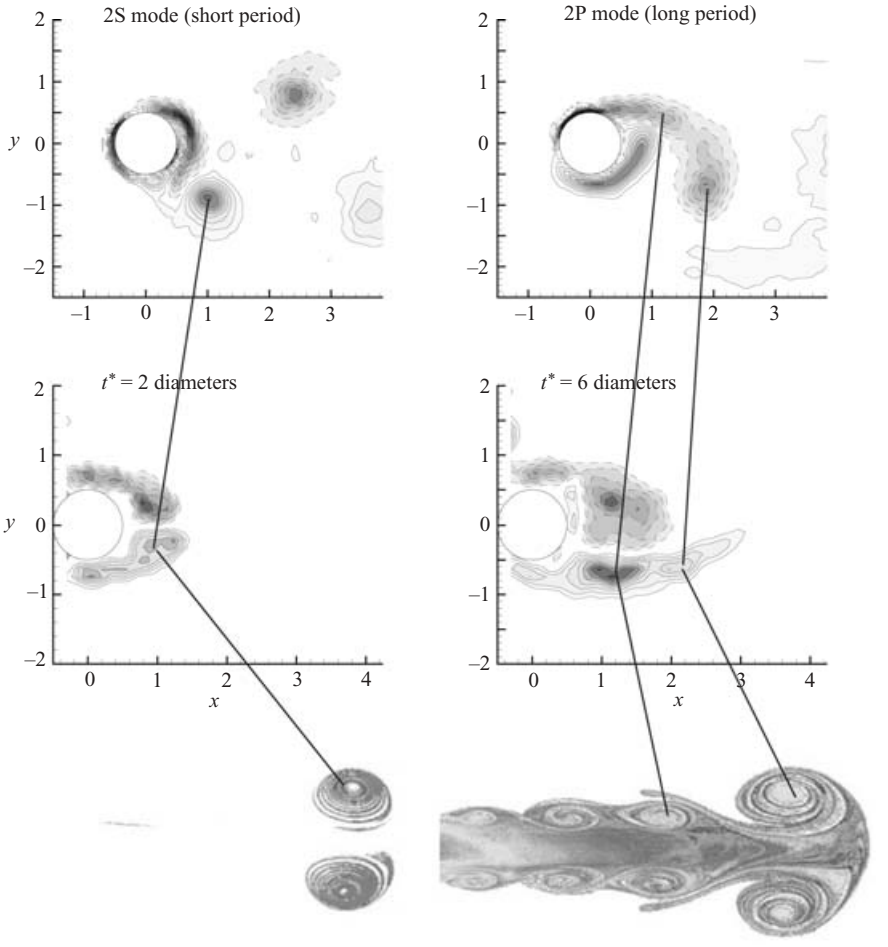

FIGURE 10. Comparison of vortex morphology for three different forming vortices. Lines are drawn for comparison between the equivalent structures seen in the three cases.

layer. In the vortex ring, as the formation time is increased past four diameters, the extra circulation pumped into the fluid remains behind in a trailing jet-like shear layer. In the starting cylinder, after the cylinder moves more than four diameters from rest, the wake destabilizes, becomes asymmetrical, and one vortex elongates. This vortical structure splits off a vortex, with the remaining circulation trailing back to the cylinder. In the forced oscillating cylinder, as the cylinder oscillation period increases somewhat beyond the Strouhal period, the extra circulation remains behind in a trailing-shear-layer structure connecting the main vortex with the cylinder. Measurements of the vortex circulation in the oscillating cases showed that there is in fact little difference in the circulation of the shed vortex at short or long oscillation period. The extra circulation is ending up in the trailing shear layer. Consequently, it is believed that the vortex formation process also affects the oscillating cylinder case, causing a straightforward transition in the wake from compact vortices to elongated vortex and trailing-shear-layer structures. Other consequences of formation will be discussed below.

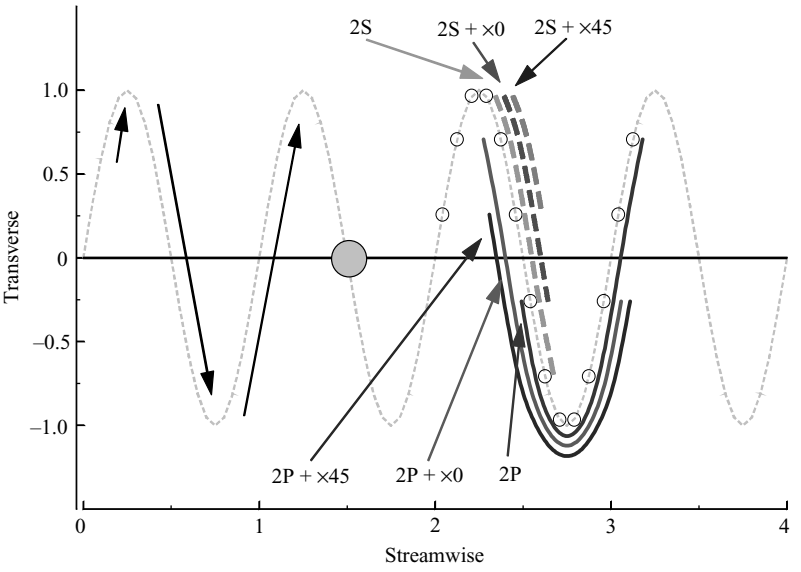

FIGURE 11. Phases of motion when a vortex is attached to the cylinder. Plotted are the times when a vortex is attached to the upper side of the cylinder. (The sinusoid represents the motion of the cylinder through space.) The dashed lines represent the higher frequency case (0.84 Strouhal periods) and the solid lines, the lower (1.2 Strouhal periods). In all cases, the vortex begins forming on the falling stroke (leeward side). The wake appears to flip at lower frequency because the vortex sheds on the rising stroke.

5.1. *Effect of the formation process on the apparent phase of the wake*

An interesting consequence of the change in vortex formation as the oscillation period crosses the Strouhal period is its effect on the phase of the wake (relative to the motion of the cylinder). As mentioned in the introduction, an oft-noted observation is that the lift forces on the cylinder flip in phase when the forced oscillation period varies across the nominal Strouhal period. Researchers have noticed that the wake, as well, appears to have flipped phase across this transition (i.e. the wake appears to be upside down at the same part of the motion cycle) (Ongoren & Rockwell 1988). However, by plotting the phase time that the vortex remains attached the cylinder, the role of formation in this phase change is evident. Since the vortex is only fed by the cylinder, its formation time is intimately related to the time it is attached to the cylinder. Figure 11 plots the attached times for a variety of cases. The lines indicate phase of the motion when a vortex is attached to the upper side of the cylinder (in our case, vortices of negative circulation). Let us first concentrate on the upper dashed lines – these are for the higher frequency/lower formation time cases. Notice that the lines start and end on the falling stroke, indicating that a vortex has formed on the leeward side and shed before reaching the transverse minima of motion. However, for the lower solid lines (lower frequency/longer formation time cases), the behaviour has changed. Although the vortex has begun to form on the leeward side, as before, the increased formation time means that the vortex ends up shedding on the opposite stroke. In all cases, the vortex begins to form on the leeward side. But at longer formation times, the vortex does not shed until after the cylinder changes direction. Hence the wake appears to have switched phase.

That the flipping of the phase of the wake is enough to cause the phase transition is illustrated below. We start with the impulse formulation, but ignoring the added mass force,

$$\boldsymbol{F} = \frac{\mathrm{d}}{\mathrm{d}t}\left(\rho \int \boldsymbol{x} \times \boldsymbol{\omega}\, \mathrm{d}V\right). \tag{5.1}$$

Taking the component in the lift direction, and considering only the most dominant vortex, this becomes

$$\text{lift} \approx -\frac{\mathrm{d}}{\mathrm{d}t}(\rho x \Gamma) = -\rho(\Gamma \dot{x} + x\dot{\Gamma}) \tag{5.2}$$

where Γ refers to the circulation of that vortex and x its position downstream from the cylinder. Since both x and the circulation are increasing during the formation process, the sign of the lift force is determined by the sign of Γ relative to the motion of the cylinder. To obtain positive coupling (between the motion of the cylinder and the lift force), the dominant vortex in the wake should be negative on the rising stroke. In other words the lift force and the transverse velocity must have the same sign. Exceeding the critical formation time causes the wake to move into the opposite-stroke shedding state which results in a positive coupling between the wake forces and the cylinder motion.

It is worthwhile to emphasize that these formation time effects are not the same as phase shifting. The magnitude of perturbation involved in our experiment is quite large. Whereas for small perturbations one might think of this problem as a forced linear oscillator (with the cylinder motion forcing the wake), that kind of model does not work here. For instance, Lofty & Rockwell (1993) show a good example of a linear perturbation on the wake. Their model of the phase clock is quite reasonable for their kind of perturbation. (They used a flapping trailing edge to modify the oscillating wake of a bluff body.) However, to borrow their clock model, our experiment would be one where the clock is so perturbed that it does not make 12 hour cycles anymore. At shorter formation times, we are interrupting the normal formation time; it is as if the clock only runs from 12 to 8 before resetting. Likewise at longer formation times, the formation is prolonged as if the clock ran past 12 to 4 before resetting. Our work shows that the wake appears to flip phase because the reset point of the clock appears to be on opposite sides of the clock, even though the starting phase time might be the same. And this results simply from the relationship between formation time and the forcing period.

In a sense, it is a string of coincidences that leads to the strong coupling of the structure to its wake. Since a passive structure cannot send net energy to the wake, the structure must necessarily oscillate at frequency less than or equal to the frequency of the wake. Therefore a passive structure selects lower frequencies, which are necessarily at longer formation time. This leads to a change in the morphology of the wake which allows the vortices to remain attached long enough to switch the phase of shedding and hence the forcing. If it were not for the changing morphology as the critical formation time is exceeded, the strong fluid–structure coupling might not materialize since the fluid forcing and the structure motion would have the wrong phase relationship.

5.2. *From whence comes the pairing mode?*

The question still remains – what role does the transition to the 2P state have to do with the vortex formation process? The 2P mode is where two pairs of vortices are formed and shed as dipole pairs per side per cycle. (See Williamson & Roshko

1988). To answer this question, it is worth a quick aside on the effect of streamwise acceleration on the formation process. By superimposing streamwise acceleration on top of the regular transverse motion, the rate of formation can be altered. If the cylinder were to accelerate forward during formation, there would be less time for the vortex to form before it sheds. Since the 2P mode appears on the long formation side, we believe there is a connection between long formation and the appearance of the 2P mode. Upon closer examination, it appeared to us that the extra vortex formed in the 2P mode forms on the long shear layer that is characteristic of long formation time wakes. In the framework of formation time, our supposition is that the second vortex in the pair forms from a secondary roll-up of the connecting shear layer in the sense of Kelvin–Helmholtz instabilities, and hence is just a by-product of long formation time. For example, in figure 9, if the cylinder motion did not include the streamwise component, the wake would be the classic 2P mode. But with the small streamwise forward acceleration, the pairing mode disappears. The forward motion during figure-eight motions cuts short the formation process before the second vortex can appear.

However, if this were true, then the 2P state should reappear if the figure-eight motion were run backwards. In this case (streamwise motion at 180° phase difference to the transverse), the cylinder would run back towards the vortex during the formation process, prolonging the formation process. If our supposition is correct, then this reverse motion during formation should bring about the return of the 2P mode. As shown in figure 12, the actual result is more interesting. Rather than simply forming two vortices per side, the prolonged formation time allows a third vortex to form during the same cycle. (The first two correspond to the pair of vortices formed in the 2P state.) It would indeed appear that the pairing state is most likely a result of extended formation (longer than normal shedding period) rather than a mode change in and of itself. Alternatively, the appearance of extra vortices is a quick way of seeing that extended formation is occurring, although not uniquely so. These three types of vortex groupings are summarized in figure 13, where the forward and backward accelerations are the same magnitude, differing only in sign. Note the general similarity of the vortex patterns (aside from number) and the same curvature of the long shear layer. In a straightforward way, the formation time is linked to the formation of extra vortices during shedding, which makes it appear that a mode transition has occurred. So while the mode shift to 2P is a useful diagnostic in looking at formation time, we believe the formation time effect is more fundamental to processes in the near wake.

It is also worth noting that the effect is the reverse of what one might expect if the single vortex of the 2S mode is split into two to form the pair in the 2P mode. The amount of strain on the vortex should decrease in the 180° phase case (where the cylinder goes downstream during formation), yet the number of vortices formed increases. By using the idea of vortex formation time, an alternative perspective on the mode transition in the wake of the oscillating cylinder can be presented.

6. Conclusions

As important as vortices are in bluff-body flows, how those vortices form (and how long it takes to form them) is equally important. The vortex formation described in Gharib *et al.* (1998) has been found to have bluff-body analogues, and has been shown to have a significant effect on the development and nature of the flow. Much like the formation process defines a characteristic time for vortex ring flows, so there are also characteristic formation times in bluff-body flows.

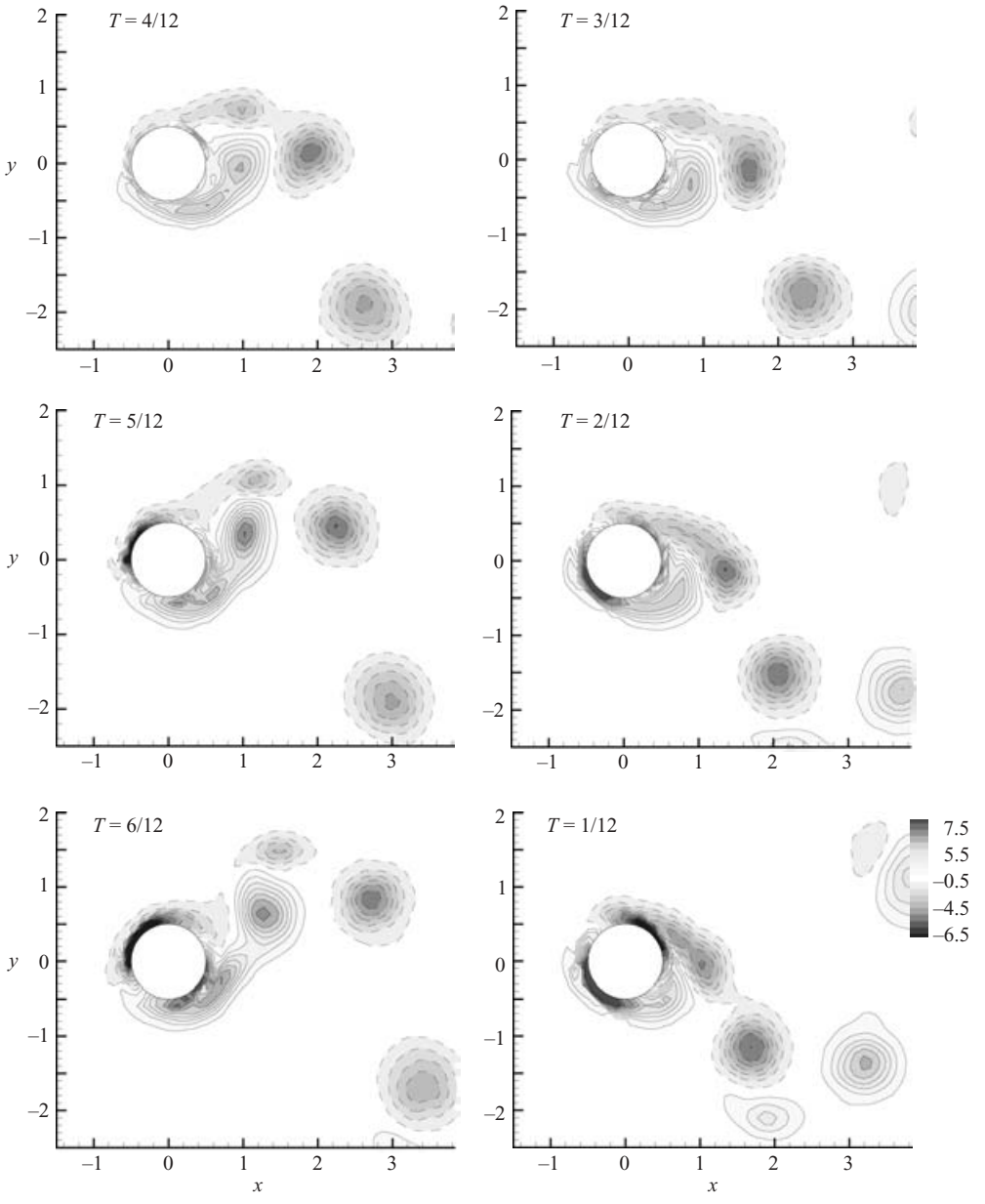

FIGURE 12. Wake of an oscillating cylinder for the upper half of motion. T refers to the phase time (from 1/12 to 12/12). Reynolds number is 990, transverse period is 1.2 the nominal Strouhal period, transverse amplitude is 0.5 diameters, streamwise amplitude is 0.1 diameters, and the relative phase between the two is 180°. Contours are non-dimensional vorticity levels of -8.5, $-7.5 \ldots 8.5$.

For the starting cylinder, this time seems to signal the onset of asymmetry in the wake. It is this symmetry breaking that eventually leads to the von Kármán vortex street pattern. Otherwise the wake would remain symmetrical and vorticity would be diffused from the wake, as opposed to being shed. At early times, the wake is symmetrical, and the vortices do not interact strongly. Around a time of four

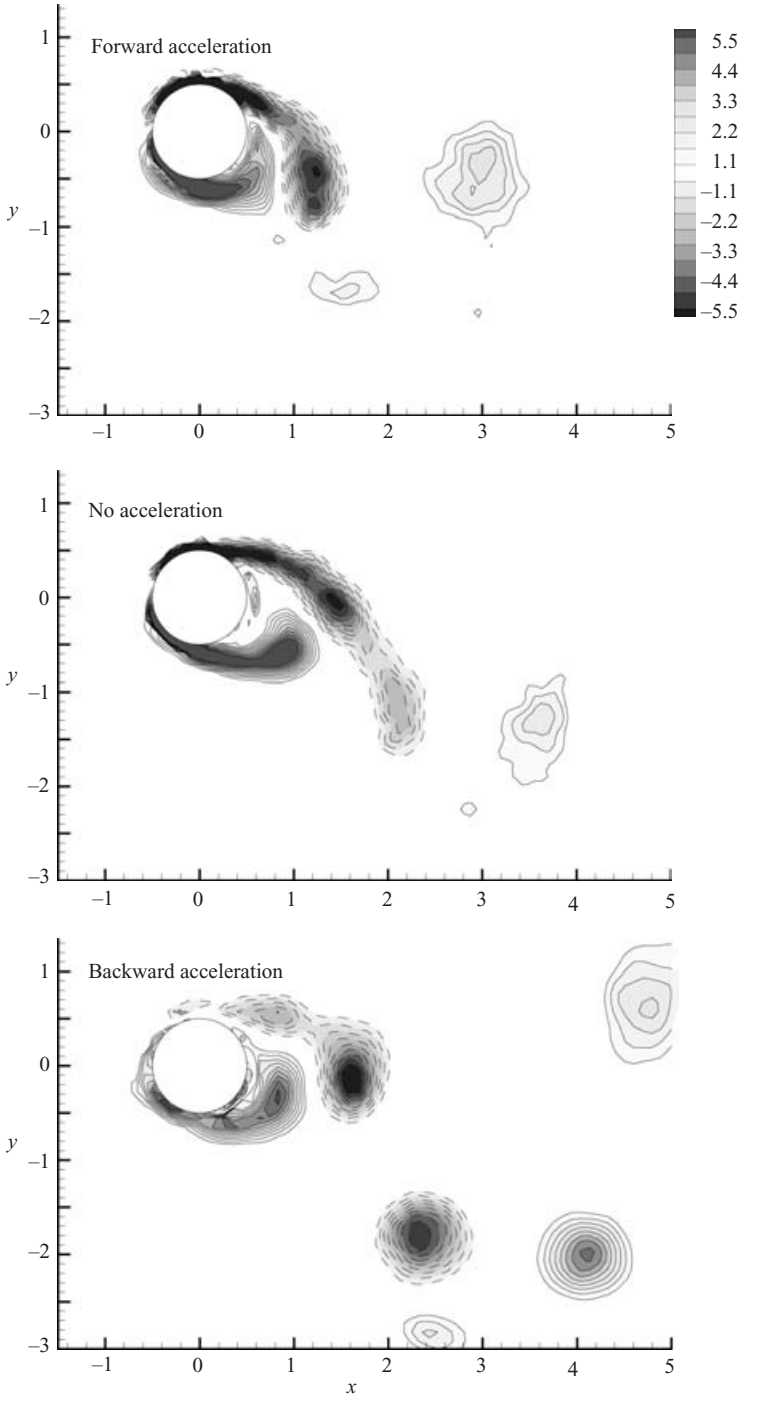

FIGURE 13. Comparison of the wake of an oscillating cylinder. All three cases have the same transverse oscillation frequency. Forward acceleration means that the cylinder is accelerating into the free stream at the extrema of motion. Note that the general morphology is preserved, but the change in formation time by the streamwise motion changes the number of vortices formed per cycle. Contours are non-dimensional vorticity levels of -5.5, $-4.95 \ldots 5.5$.

diameters, the wake appears to sharply increase the degree to which it is asymmetrical. Also at time four, the wake vortices have the same circulation as the vortex that is first shed, leading us to believe that a critical circulation has been reached. The asymmetry in the wake continues to grow from there until shedding occurs.

For the cylinder undergoing forced oscillations, the characteristic formation time marks the switch in the phase of the wake, relative to the motion of the cylinder. At higher oscillation frequencies, the vortices are formed in less than the critical time and hence form and shed on the same stroke of the cylinder motion. At lower oscillation frequencies, the vortex formation stretches past the critical time, leading to formation and shedding occurring on opposite strokes. This accounts for the observed phase change in the wake. In addition, the phase change allows the wake and the cylinder motion to positively couple. Formation time effects were also shown to underlie the '2P' mode of vortex shedding. It is believed that prolonging formation allows time for the trailing-shear-layer structure to have a secondary (or even tertiary) roll-up, leading to the formation of additional vortices per cycle.

That said, the detailed mechanisms by which these vortices reach saturation remains to be discovered. For the vortex ring, the critical time corresponds to a minimum in the energy of the vortex, after which it becomes favourable for the vortex to move downstream. Whether a similar mechanism underlies vortex shedding has not been determined. Nevertheless, the wake of the circular cylinder seems to be paced by a vortex formation time. And bearing that in mind appears to clarify some of the behaviour of those wakes.

The authors would like to thank the Office of Naval Research (grant numbers N00014-93-1144 and ONR-N00014-94-1-0793) for their generous support, and Professors A. Roshko and A. Leonard for helpful discussions and useful advice.

REFERENCES

Bishop, R. E. D. & Hassan, A. Y. 1964 The lift and drag forces on a circular cylinder oscillating in a flowing fluid. *Proc. R. Soc. Lond.* A **277**, 51–75.

Bouard, R. & Coutanceau, M. 1980 The early stage of development of the wake behind an impulsively started cylinder from $40 < Re < 10^4$. *J. Fluid Mech.* **101**, 583–607.

Brika, D. & Laneville, A. 1993 Vortex-induced vibrations of a long flexible circular cylinder. *J. Fluid Mech.* **250**, 481–508.

Carberry, J., Sheridan, J. & Rockwell, D. 2001. Forces and wake modes of an oscillating cylinder. *J. Fluids Struct.* **15**, 523–532.

Gharib, M., Rambod, E. & Shariff, K. 1998 A universal time scale for vortex ring formation. *J. Fluid Mech.* **360**, 121–140.

Govardhan, R. & Williamson, C. 2001 Mean and fluctuating velocity fields in the wake of a freely oscillating cylinder. *J. Fluids Struct.* **15**, 489–502.

Gu, W., Chyu, C. & Rockwell, D. 1994 Timing of vortex formation from an oscillating cylinder. *Phys. Fluids.* **6**, 3677–3682.

Honji, H. & Taneda, S. 1969 Unsteady flow past a circular cylinder. *J. Phys. Soc. Japan* **27**, 1668–1677.

Koumoutsakos, P. & Leonard, A. 1995 High-resolution simulations of the flow around an impulsively started cylinder using vortex methods. *J. Fluid Mech.* **296**, 1–38.

Lofty, A. & Rockwell, D. 1993 The near-wake of an oscillating trailing edge: mechanisms of periodic and aperiodic response. *J. Fluid Mech.* **251**, 173–201.

Ongoren, A. & Rockwell, D. 1988 Flow structure from an oscillating cylinder. *J. Fluid Mech.* **191**, 197–246.

Parkinson, G. 1989 Phenomena and modelling of flow-induced vibrations of bluff bodies. *Prog. Aerospace Sci.* **26**, 169–224.

Pullin, D. 1979 Vortex ring formation at tube and orifice openings. *Phys. Fluids* **22**, 401–403.

Saffman, P. 1992 *Vortex Dynamics*, pp. 147–52. Cambridge University Press.

Sarpkaya, T. 1979 Vortex-induced oscillations: a selective review. *J. Appl. Mech.* **46**, 241–258.

Willert, C. E. & Gharib, M. 1991 Digital particle image velocimetry. *Exps. Fluids* **10**, 181–193.

Williamson, C. H. K. & Govardhan, R. 2004 Vortex-induced vibrations. *Annu. Rev. Fluid Mech.* **36**, 413–455.

Williamson, C. H. K. & Roshko, A. 1988 Vortex formation in the wake of an oscillating cylinder. *J. Fluids Struct.* **2**, 355–381.